NTIA-REPORT-78-8

Estimates of the Atmospheric Transfer Function at SHF and EHF

E. J. Dutton
H. T. Dougherty

U.S. DEPARTMENT OF COMMERCE
Juanita M. Kreps, Secretary

Henry Geller, Assistant Secretary
for Communications and Information

August 1978

TABLE OF CONTENTS

LIST OF FIGURES

LIST OF TABLES

ESTIMATES OF THE ATMOSPHERIC TRANSFER FUNCTION AT SHF AND EHF

by

E. J. Dutton and H. T. Dougherty*

ABSTRACT

Known theory is applied to examine the channel transfer function for earth/space propagation paths through the atmosphere and over the frequency range from 10 to 350 GHz. The associated attenuation and phase-delay characteristics are separated into the contributions of the clear-sky, clouds, and rainfall. From the available meteorological data, the total path attenuation and phase-delay is estimated over the frequency range from 10 to 45 GHz for selected values of the initial elevation angles from a ground station near Washington, DC.

The associated attenuation coefficients (dB/km) and phase-delay coefficients (rad/km) attributable to the clear air, clouds, and rainfall are also described for frequencies up to 350 GHz.

Key Words: Atmospheric attenuation, atmospheric phase delay, microwave frequencies, millimeter waves, clear-air effects, effects of clouds, effects of rainfall.

1. INTRODUCTION

With the approach of the General World Administrative Radio Conference in 1979 (GWARC-79), there has been an increasing interest in the further development of frequency allocations above 10 GHz. One factor of concern in any expansion of radio services into this relatively unused portion of the radio spectrum is the role of the atmosphere. The purpose of this report is to present some quantitative estimates of the characteristics of the atmosphere that are significant for radio wave propagation and telecommunication system performance above 10 GHz and below 350 GHz.

---

*The authors are with the Institute for Telecommunication Sciences, National Telecommunications and Information Administration, U. S. Department of Commerce, Boulder, CO 80303.

1.1. The Channel Transfer Function

We may express the relevant characteristics in terms of an atmospheric channel transfer function

$$H(f) = A(f) \exp[-i\Phi(f)], \tag{1}$$

a function of the radio transmission frequency f. The $\Phi(f)$ is the phase delay experienced by the radio wave propagating through the medium. The amplitude function A(f) expresses the losses suffered by the same radio wave and may be related to the signal attenuation, $\tau_r(f)$ in decibels, by

$$A(f) = \frac{1}{r} \exp[-0.11513\ \tau_r(f)] \ . \tag{2}$$

Here, the r is the propagation path length along which the attenuation (caused by absorption and scattering) is experienced.

The atmospheric channel transfer function is, of course, time variant with random fluctuations such as turbulence fluctuations that are well treated elsewhere (Ishimaru, 1972). Here, we approximate the atmosphere and its transfer function as time invariant, at least for the short time intervals that are of interest for the transmission at high information rates.

To the simplified channel transfer function of (1), one would normally add the additive and multiplicative noise of interference sources of concern to telecommunication system designers (Linfield, 1977). Such additional considera-ations are, however, beyond the scope of this report. We are restricting this presentation to estimates of the simple channel transfer function.

1.2. The Attenuation Function

The total atmospheric attenuation at frequency f can be expressed in decibels as

$$\tau_r(f) = \tau_o(f) + \tau_w(f) + \tau_c(f) + \tau_p(f), \tag{3}$$

where

$\tau_o(f)$ is for the absorption (in decibels) by atmospheric oxygen,

$\tau_w(f)$ is for the absorption (in decibels) by atmospheric water vapor,

$\tau_c(f)$ is for the attenuation (in decibels) caused by clouds, and

$\tau_p(f)$ is for the attenuation (in decibels) caused by precipitation.

The r subscript on the left-hand side of (3) is a reminder that attenuation is determined for the entire path although the terms on the right-hand side of (3) each have an associated ℓ, not necessarily equal to r or each other. For example, for the oxygen and water vapor terms of (3), the appropriate common ℓ is that portion of r within the gaseous (clear-sky) atmosphere. The appropriate ℓ for the cloud attenuation term is that portion of r within the cloud. The appropriate ℓ for the precipitation term of (3) is that portion of r within the region of precipitation.

Figure 1 is an over-all view of the atmospheric attenuation coefficients (in decibels per kilometer) at sea level, adapted from Zuffrey (1972); see also CCIR (1978). The continuous-line curve is a plot of the attenuation coefficient for the gaseous (clear-sky) atmosphere (for a temperature of 20°C and 7.5 gm/m^3 of water vapor density). For frequencies below about 350 GHz, this clear-sky attenuation is primarily due to the absorption of radio energy by oxygen and water vapor, as in (3). The dot-dash curve of attenuation coefficient versus frequency is that for cloud or fog (with 0.1 gm/m^3 of water in droplet form). The dotted curves are the attenuation coefficients for various rainfall rates. The 150 mm/hr is an extremely high rainfall rate rarely encountered in the U.S.; the 25 mm/hr is a moderate rainfall rate exceeded in the southeastern U.S. for a cumulative total of about 8 hrs/yr; the 0.25 mm/hr is an extremely light rainfall.

Since the gaseous atmosphere is always present, the clouds or fog commonly present, and the various rainfall rates only intermittently present, their relative importance can be obscured by the presentation of Figure 1. Further, the appropriate ℓ for the gaseous atmosphere will correspond to the entire propagation path length within the atmosphere. For the highest rainfall rates, the associated ℓ can be much less.

1.3. The Phase Delay Function

There is, of course, the same association of ℓ's with the sources of the radio wave phase delay. The total phase delay at frequency f can be expressed in radians as

$$\Phi_r(f) = k_o r + \Phi_N(f) + \Phi_c(f) + \Phi_p(f) \quad , \tag{4}$$

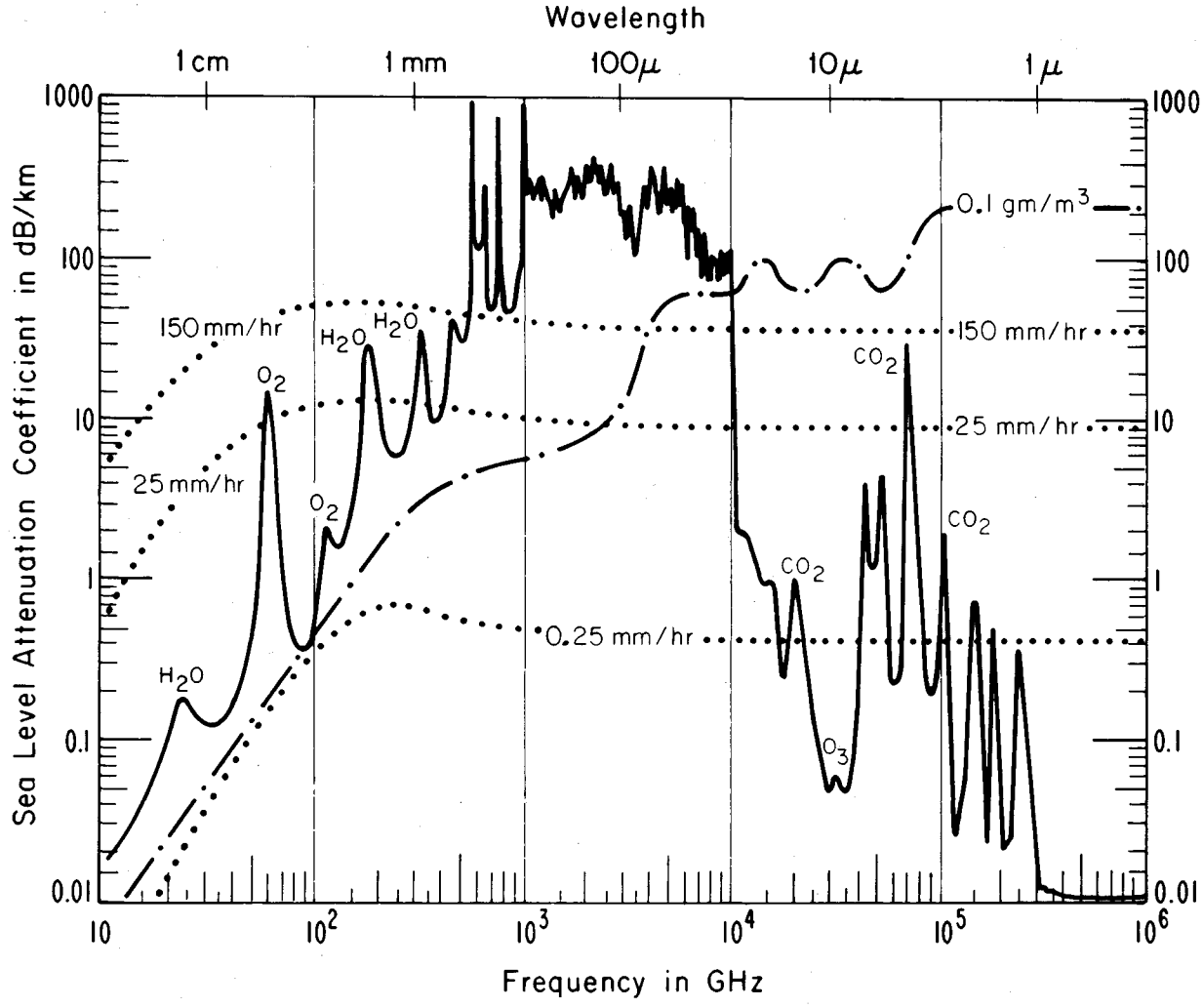

Figure 1. Sea-level attenuation coefficients, in decibels per kilometer, versus frequency for: the gaseous atmosphere (the continuous line curve for 20°C temperature and water vapor density of 7.5 gm/m^3); clouds (the dot-dash curve for water droplets 0.1 gm/m^3), and various rainfall rates (the dotted curve).

where

k_o is the free-space wave number in radians per kilometer,

$\Phi_N(f)$ is the clear-sky phase delay (in radians) caused by refraction,

$\Phi_c(f)$ is the phase delay (in radians) caused by clouds, and

$\Phi_p(f)$ is the phase delay (in radians) caused by precipitation.

The clear-sky phase delay can be separated into two terms

$$\Phi_N(f) = \Phi_{Na} + \Delta\Phi_N(f) \quad , \tag{5}$$

where

Φ_{Na} is the non-dispersive (independent of frequency) term, and

$\Delta\Phi_N(f)$ is the dispersive (frequency-dependent) term.

This dispersive term is generally the smaller of the two terms, except near resonance (frequency) lines.

1.4. Transfer Function Limitations

When one reviews the present understanding of the various phenomena involved in radio wave propagation through the atmosphere, it is clear that progress has been non-uniform. For example, the attenuation and phase delay caused by the gaseous atmosphere has been the subject of concentrated fundamental efforts that have produced a theoretical treatment that is well formulated and experimentally verified for frequencies below about 130 GHz.

There are five major molecular resonant frequency lines in the 10 to 350 GHz range, in addition to numerous minor lines attributable to atmospheric gases (Lukes, 1968). These major lines are:

a) the water-vapor resonance line in the vicinity of 22 GHz;

b) the oxygen resonance lines in the vicinity of 60 GHz;

c) the oxygen resonance line in the vicinity of 119 GHz;

d) the water-vapor resonance line in the vicinity of 183 GHz; and

e) the water-vapor resonance line in the vicinity of 323 GHz.

The absorption and phase delay characteristics of the first three resonance lines (a, b, and c above) have been extensively studied (Liebe, 1969;

Liebe, et al., 1977). Further, estimates of the attenuation and phase delay characteristics of molecular oxygen resonances in the vicinity of both 60 and 119 GHz have been presented for the earth/space systems (Liebe, et al., 1977; Liebe and Hopponen, 1977). An approximate formulation for both the attenuation and phase delay caused by oxygen is available for computer-programming purposes over the range of 50 to 120 GHz (Ott and Thompson, 1976).

Similarly, for the attenuation and phase delay caused by raindrops, the appropriate theory must be modified as the Rayleigh condition (that the raindrop dimensions are small relative to the radio wavelength) becomes less applicable for frequencies exceeding about 45 GHz. Further, the polarization-dependent effects of the non-sphericity of raindrops, their tilt angles, and the vertical structure of rainstorms all combine to create increasing uncertainties above about 45 GHz.

For these reasons we have divided our presentation according to two frequency ranges:

1) At 10 to 45 GHz, there is sufficient relevant data to permit some extrapolation of theory and to determine estimates of total attenuation and phase delay for earth/space systems.

2) At 45 to 350 GHz, the situation is mixed. For clear-sky conditions the prediction procedures from 45 to 130 GHz are so well developed that the attenuation and phase delays for earth/space systems are already available in the literature. For rainfall, the available data and theory can be applied to about 80 GHz. Above 130 GHz, the theory is sufficiently undeveloped and the experimental data is so limited that of the attenuation coefficient (dB/km) and phase-delay coefficients (rad/km) have only been estimated.

2. ATTENUATION AND PHASE DELAY ESTIMATES FOR 10 TO 45 GHz

The attenuation function for the entire propagation path is given in (3) in terms of contributory components, each of which is a path-integrated quantity. For example, the attenuation due to the oxygen in the atmosphere

is given in decibels by

$$\tau_o(f) = \int_o^r \alpha_o(f)\, dL \quad . \tag{6}$$

The quantity $\alpha_o(f)$ is the absorption coefficient of oxygen per kilometer of path length within the atmosphere. For the attenuation due to water vapor in the atmosphere, $\tau_w(f)$, there is a corresponding $\alpha_w(f)$. For the attenuation by cloud, $\tau_c(f)$, the corresponding attenuation coefficient per kilometer of path length within cloud is identified as $\alpha_c(f)$. For the attenuation by precipitation, $\tau_p(f)$, the corresponding coefficient $\alpha_p(f)$, is attenuation per kilometer of path length through the precipitation region.

2.1. Clear-Sky Attenuation

The attenuation due to clear-sky conditions (i.e., due to absorption by the gaseous constituents of the atmosphere) is that indicated as the sum of two terms in (3), $\tau_o(f)$ due to oxygen and $\tau_w(f)$ due to water vapor. For the frequency region 10 to 45 GHz, Van Vleck (1947a) gives a formulation for the oxygen absorption per unit length, $\alpha_o(f)$, as

$$\alpha_o(f) = \frac{0.34f^2}{c^2}\left[\frac{\Delta\nu_1}{\frac{f^2}{c^2}+\overline{\Delta\nu}_1^2} + \frac{\Delta\nu_2}{(2+\frac{f}{c})^2+\overline{\Delta\nu}_2^2} + \frac{\Delta\nu_2}{(2-\frac{f}{c})^2+\overline{\Delta\nu}_2^2}\right] \tag{7}$$

The $\Delta\nu_1$ and $\Delta\nu_2$ are line widths whose values may be found in Bean and Dutton (1968), and c is the velocity of light in vacuo. Van Vleck's (1947b) form for the water vapor absorption per unit length $\alpha_w(f)$, is given as

$$\alpha_w(f) = \alpha_{w1}(f) + \alpha_{w2}(f) \ , \tag{8a}$$

where

$$\alpha_{w1}(f) = \left[\frac{0.0035f^2w}{c^2}\left[\frac{\Delta\nu_3}{(\frac{f}{c}-\frac{1}{1.35})^2+\overline{\Delta\nu}_3^2} + \frac{\Delta\nu_3}{(\frac{f}{c}+\frac{1}{1.35})^2+\overline{\Delta\nu}_3^2}\right]\right. \tag{8b}$$

$$\alpha_{w2}(f) = \frac{0.05f^2\Delta\nu_4}{c^2} \tag{8c}$$

In (8b) and (8c), w is the water vapor density (g/m^3) and $\Delta\nu_3$ and $\Delta\nu_4$ are line widths whose values also can be found in Bean and Dutton (1968). It should be emphasized that the values of $\Delta\nu_i$, i=1,2,3,4 in (7) to (8c) are fits to experimental atmospheric data, thus assuring some validity of the formulations for use in practical applications. Other fits (Liebe, 1969) are available for the absorption coefficients $\alpha_o(f)$ and $\alpha_w(f)$, but the above Van Vleck-Weiskopf fits, appear to be the best below 50 GHz.

A number of meteorological parameters are required to assess the values of $\alpha_o(f)$ and $\alpha_w(f)$. They are the atmospheric pressure, P, temperature, T, and water vapor density w, and their gradients, ∇P, ∇T, and ∇w which determine the values of $\Delta\nu_1$, $\Delta\nu_2$, and $\Delta\nu_3$ through the atmosphere. In the atmosphere, it can be shown that the significant gradient is in the vertical direction for P and T. For water vapor density, w, this is less certain, especially when the atmosphere is turbulent. Because of the sparsity of meteorological gradient data, however, we shall generally be forced to assume horizontal homogeneity of P, T, and w when assessing attenuation and dispersion effects. Thus, given the elevation angle, θ_o, of the antenna and some vertical profile information on P, T, and w, one can construct a rather detailed picture of the total clear-sky attenuation in (6) by integrating $\alpha_o(f)$ and $\alpha_w(f)$ along the exact path described by the refractive index (Bean and Dutton, 1968).

2.2. Attenuation By Clouds

Atmospheric clouds (precipitating and non-precipitating) were modeled by Dutton (1968) on the basis of Diermendjian's (1963) dropsize density function

$$n(\rho) = a_c \rho^6 \exp(-b_c \rho) \ . \tag{9a}$$

Here, $n(\rho)$ is the number of drops whose radius, ρ, lies between ρ and $\rho + d\rho$, and a_c and b_c are constants depending upon the cloud type. For the "thickest" clouds (cumulus congestus), those with the greatest potential for causing attenuation,

$$a_c \cong 1.16 \ cm^{-3} \ \mu^{-7} \tag{9b}$$

$$b_c \cong 1.1 \ \mu^{-1} \ , \tag{9c}$$

for $n(\rho)$ measured in $cm^{-3}\ \mu^{-1}$, and ρ in microns (μ). The expression (9a) is, essentially, a non-normalized gamma-distribution density function. If we assume (9a), (9b), and (9c) apply to all cloudiness along the path (a worst-case situation) then, using the Rayleigh-region approximations, we can obtain the attenuation coefficient for clouds, the attenuation per kilometer,

$$\alpha_c(f) = 0.560 \frac{fD}{(C+2)^2+D^2} \quad . \tag{10}$$

In (10), the frequency is in gigahertz and the C and D are the real and imaginary parts of the dielectric coefficient of water,

$$\varepsilon = C-iD \quad . \tag{11}$$

The dielectric constant of (11) is related to the index of refraction of water, m, assuming no magnetic effects, by

$$m = \sqrt{\varepsilon} \quad . \tag{12a}$$

Thus, m is also a complex number,

$$m = m' - im'' \quad . \tag{12b}$$

In spite of the terminology "dielectric constant", the C and D, and hence m' and m'' are frequency dependent.

Goldstein (1951), has indicated that a mathematical relationship, between and frequency, called the Debye formula, represents a good fit to data for frequencies up to about 30 GHz used in SHF rainfall-effect computations. At EHF, however, not that many data have been taken. Using a relative wealth of data at optical frequencies, Ray (1972) has essentially "blended in" the EHF region by joining the optical and SHF results. As a consequence, he obtains curves for EHF that are closely approximated by the Debye formulation.

2.3. Attenuation By Precipitation

The major contributor to attenuation by precipitation is that attributable to rainfall. For telecommunication purposes and for studying long-term effects, Rice and Holmberg (1973) have treated all precipitation as if it were effectively rainfall. The attenuation coefficient for rain, $\alpha(f,h)$ in decibels per kilometer, is a function of the transmission frequency f

and the elevation h of the point of observation above the surface (Dutton and Dougherty 1973)

$$\alpha(f,h) = a_1(f)\ [L(h)]^{b_1(f)} \quad , \tag{13a}$$

where

$a_1(f)$ is a frequency-dependent coefficient (dB/km) determined (Dutton and Dougherty, 1973) with data from 1.29 to 94 GHz (Crane, 1966);

$b_1(f)$ is a frequency-dependent exponent also determined by regression analysis of Crane's data (1966);

$L(h)$ is liquid water content of the rainfall (g/m^3) at a height h above the surface.

The vertical structure of the liquid water content, $L(h)$, is determined by rainfall rate R_o at the surface (h=0) and the mix of rainfall types (Dutton, 1977a)

$$L(h) = \beta L_c(h) + [\ 1 - \beta]\ L_s(h) \quad , \tag{13b}$$

where

β is the predicted convective ratio (the ratio of convective rainfall to total rainfall (Rice and Holmberg, 1973);

$L_c(h)$ is the convective rainfall vertical structure of liquid-water content [i.e., the dominant term of (13b) for the highest rainfall rates] (Dutton, 1967);

$L_s(h)$ is the stratiform rainfall vertical structure of liquid-water content (i.e., the dominant term of (13b) for the lighest rainfall rates) (Dutton, 1971).

These vertical structures are predicted from the surface values of rainfall rate, pressure, temperature, and the cloud- top height. These vertical structures also include the Marshall-Palmer (1948) raindrop size distribution

$$n(\rho,h) = A(h)\ \exp[-\rho B(h)] \quad , \tag{14a}$$

where

$$B(h) = 8.2[R(h)]^{-0.21} \ \text{mm}^{-1} \quad . \tag{14b}$$

Here, $n(\rho,h)$ is the number of raindrops with radii between ρ and $\rho + d\rho$ millimeters at an elevation h above the surface. For terrestrial systems, $h \approx 0$ and $R(h)=R_o$ and $A = 16000\ mm^{-1}m^{-3}$. For earth/space systems, however, we approximate the dropsize distribution by again using the surface rainfall rate R_o to determine B, but then we take A to be only $8000\ mm^{-1}m^{-3}$ (Dutton, 1977a).

Since rainfall also has a horizontal structure, especially for high rainfall rates, the point-rainfall statistics are converted to path-rainfall statistics by means of an empirical probability-modification factor (Dutton 1977a).

Predictions of surface point-rainfall one-minute rates, $R_1(p)$, in Europe and the U.S.A. are available for specific percentages (p=1.0, 0.1, and 0.01%) of an average year; the standard deviations for the year-to-year variation of these rainfall rates are also available (Dougherty and Dutton, 1978; Dutton and Dougherty, 1979).

2.4. Total Attenuation

The total attenuation, $\tau_r(f)$ in (6), along an earth/satellite path can be computed by a FORTRAN computer program DEGP76. Required inputs to this program are: the surface point-rainfall rate, R_o, and the storm-top height, H, of the storm at the earth terminal. The point-rainfall values are available for locations in Europe (Dougherty and Dutton, 1978) and the U.S.A. (Dutton and Dougherty, 1979). The storm-top heights can be approximated from rough climatological data (Grantham and Kantor, 1967) and estimated from surface rainfall rate (Dutton et al., 1974).

The attenuation of the gaseous atmosphere, clouds, and precipitation are predicted in Figure 2 for an earth station in the vicinity of Washington, DC at an elevation angle of 27° and over the frequency range of 10 to 50 GHz. The curve identified for p=50% of all hours of an average year represents the clear-sky attenuation by the gaseous atmosphere (due to oxygen and water vapor). For $1<p\leq 20\%$, the attenuation is due to the gaseous atmosphere and clouds. Note that the "window" in the vicinity of 40 GHz for median conditions is no longer available. For $p\leq 1\%$, the attenuation is caused by the gaseous atmosphere, precipitating clouds, and rainfall. The p=1% corresponds to the light rainfall (3.4 mm/hr for the vicinity of Washington, DC); the p=0.1%

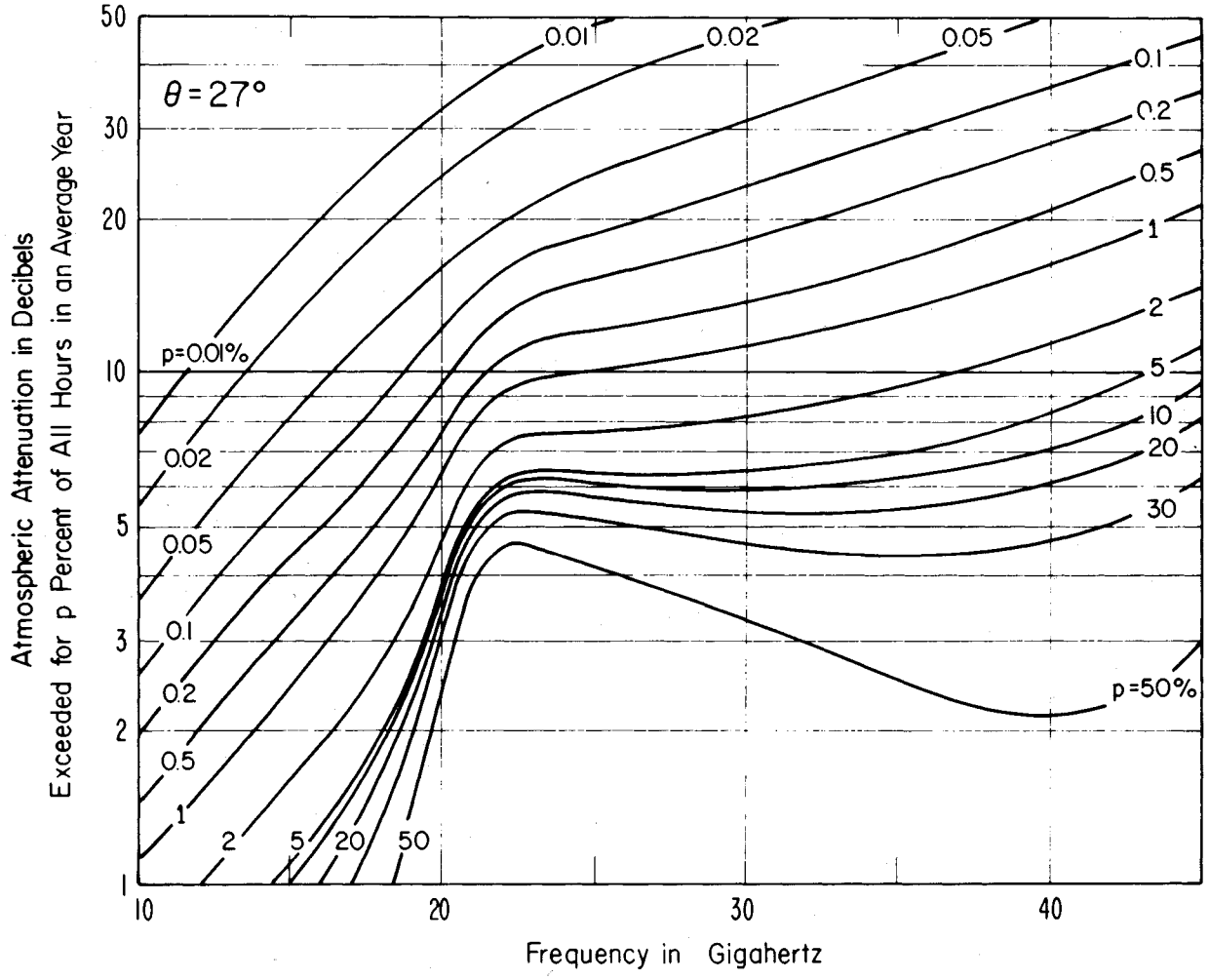

Figure 2. Predicted total attenuation, $\tau_T(f)$ in decibels, versus frequency for an earth/space path. The earth-station elevation angle is $\theta=27°$. The p=50% curve is that for clear-sky conditions. The curves for $1<p<20\%$ show the added effects of clouds. For $p\leq 1\%$ the increased attenuation is due to rainfall.

corresponds to moderate rainfall (15 mm/hr); the p=0.01% corresponds to a heavy rainfall (60 mm/hr). Although these curves are for an average year, the year-to-year variation with rainfall can be determined from the year-to-year variability (Dougherty and Dutton, 1978; Dutton and Dougherty, 1979).

For other values of the elevation angle θ and for percentages of 1% or greater, the values $\tau(p,\theta)$ may be determined from the $\tau(p, \theta=27°)$ in Figure 2 by

$$\tau(p,\theta) = 0.454 \quad \tau(p,\theta=27°) \csc\theta \ , \ p \ 1\%, \ \theta>5°. \tag{15}$$

The limitation $\theta>5°$ avoids atmospheric stratification effects and other considerations [Dutton and Dougherty, 1973]. Table I lists the total attenuation values for other elevation angles and for selected frequencies and percentages of an average year.

2.5. Phase Delays

The phase delays in (4) due to clear air, clouds, and precipitation (turbulence not included) can be shown to be given approximately by

$$\Phi_N(f) = 10^{-6}k_o \int_o^r N_a \, d\ell + 10^{-6}k_o \int_o^r \Delta N(f) \, d\ell = \Phi_{N_a} + \Delta\Phi_N(f) \tag{16a}$$

and

$$\Phi_c(f) + \Phi_p(f) = \int_o^r \phi_o(f) d\ell + 10^{-6}k_o \int_o^r m_e'(f) \, d\ell \tag{16b}$$

in radians. Here:

- N_a is the portion of the clear air refractivity which is frequency independent (Bean and Dutton, 1968),
- $\Delta N(f)$ is the dispersive or frequency dependent portion of the clear air refractivity (Liebe, 1969),
- $m_e'(f)$ is the increase in the (equivalent) refractivity of the atmosphere when it is raining (Zuffery, 1972), and
- $\phi_c(f)$ is the phase-delay coefficient (rad/km) due to clouds (precipitating or non-precipitating).

TABLE I

Atmospheric Attenuation, $\tau_r(f)$ In Decibels, For An Earth/Satellite System At Selected Frequencies, As A Function Of Initial Elevation Angle θ_o, And For p Percent Of An Average Year Near Washington, DC

Frequency	Initial Angle	Percent Of An Average Year, p				
f, GHz	θ_o, deg.	0.01	0.1	1	10	50
30	5	126.2828	77.3162	51.5731	41.1809	14.3891
	15	98.9060	35.0715	18.8881	14.8613	5.1198
	30	78.3634	18.4662	9.8492	7.7474	2.6658
	45	74.8127	13.0725	6.9739	5.4854	1.8871
25	5	89.5768	55.4456	37.0657	31.1031	13.6338
	15	69.6324	24.6697	13.5210	11.1932	4.8336
	30	55.0351	12.8984	7.0493	5.8339	2.5158
	45	52.8559	9.1308	4.9913	4.1305	1.7807
22.235	5	74.2669	47.1732	32.4512	28.5570	15.5561
	15	56.5152	20.5867	11.7833	20.2486	5.5120
	30	44.3149	10.7310	6.1416	5.3402	2.8687
	45	42.7171	7.5964	4.3483	3.7808	2.0305
20	5	58.0667	36.0622	23.9755	20.4607	9.7059
	15	45.2487	15.8805	8.7305	7.3586	3.4421
	30	35.6111	8.2701	4.5516	3.8352	1.7916
	45	34.7351	5.8544	3.2228	2.7154	1.2682
15	5	32.3261	19.8253	12.8626	10.7374	4.6102
	15	25.7103	8.7888	4.6974	3.8741	1.6453
	30	20.1184	4.5859	2.4497	2.0199	0.8570
	45	20.1902	3.2464	1.7346	1.4302	0.6067
10	5	14.0668	8.8920	6.1078	5.2957	2.7222
	15	10.3624	3.7589	2.2253	1.9122	0.9745
	30	8.3827	1.9584	1.1606	0.9971	0.5077
	45	7.4664	1.3865	0.8218	0.7060	0.3595

The first term of (16a) can be evaluated in the Washington, DC area to be (Bean and Thayer, 1963)

$$\Phi_{N_a}(f) = 10^{-6}k_o \int_o^r N_a d\ell = 2.096\times10^{4} f \csc\theta, \tag{17}$$

where θ is the earth-station antenna elevation angle and f is the transmission frequency in gigahertz. The second term of (16a) can be evaluated in radians using mean atmospheric conditions and a Lorentz line-shape (Liebe, 1969).

$$\Delta\Phi_N(f) = 10^{-6}k_o \int_o^r \Delta N(f) d\ell \cong 0.1731 \frac{f(f_q - f)}{(f_q - f)^2 + 0.0984} \csc\theta. \tag{18}$$

The frequency f is in gigahertz and f_q=22.23515 GHz is the water-vapor resonance line. The phase delay (in radians) due to cloud is

$$\Phi_c(f) = \int_o^{\ell} \phi_c(f)\, d\ell \tag{19a}$$

and

$$\phi_c(f) = 2.15(10)^{-2} f \frac{(C-1)(C+2) + D^2}{(C+2)^2 + D^2} \tag{19b}$$

in radians per kilometer. Again, the frequency f is in gigahertz and the parameters C and D are as defined by (11).

The total phase delay in excess of the first term of (4), $k_o r$ in radians, is listed for an earth-space path and for selected values of elevation angle and frequency in Table II.

3. ATTENUATION AND PHASE DELAY ESTIMATES FOR 45 TO 350 GHz

Estimates of the clear-sky attenuation and phase delay for the frequency range 45 to 130 GHz for various initial elevations ($h \leq 0$) within the atmosphere, and for zenith ($\theta=90°$) or horizontal ($\theta=0°$) paths are available in detail [Liebe, 1969; Liebe et al., 1977].

For the frequency range from 130 to 350 GHz, the major contributions to the clear-sky attenuation (absorption by the gaseous atmosphere) are primarily caused by absorption at the water-vapor resonance lines in the vicinities of

TABLE II

Atmospheric Phase-Delay, $\Phi_r(f)-k_o r$ In Radians, For An Earth/Satellite System At Selected Frequencies, As A Function Of Initial Elevation Angle θ_o, And For p Percent Of An Average Year Near Washington, DC

Frequency	Initial Angle	Percent Of An Average Year, p				
f, GHz	θ_o, deg.	0.01	0.1	1.0	10	50
30	5	20.4116	8.8890	3.2931	-1.0741*	-2.5913
	15	21.3403	5.1558	1.1949	-0.4082	-0.9619
	30	18.1930	2.7333	0.6175	-0.2156	-0.5033
	45	17.9811	1.9337	0.4365	-0.1530	-0.3566
25	5	9.7110	4.2223	-0.1861	-3.6977	-4.9234
	15	12.4790	2.9643	-0.1112	-1.3974	-1.8438
	30	11.0588	1.5502	-0.0653	-0.7337	-0.9657
	45	11.2089	1.0960	-0.0472	-0.5202	-0.6847
22.235	5	12.7872	7.8882	4.1318	1.0732	0.0027
	15	12.5897	4.1245	1.5095	0.3905	0.0010
	30	10.5597	2.1477	0.7844	0.2029	0.0005
	45	10.5282	1.5198	0.5551	0.1436	0.0004
20	5	15.7496	11.3400	8.1060	5.4033	4.4552
	15	12.8575	5.2624	3.0071	2.0189	1.6741
	30	10.2361	2.7421	1.5698	1.0563	0.8772
	45	10.0430	1.9414	1.1118	0.7484	0.6216
15	5	9.5122	6.1202	4.0114	2.0705	1.3859
	15	8.6521	2.9812	1.4733	0.7635	0.5146
	30	7.0097	1.5554	0.7674	0.3986	0.2692
	45	7.1753	1.0109	0.5433	0.2823	0.1908
10	5	7.2795	3.6210	2.2486	1.0047	0.5638
	15	6.5769	1.7123	0.8203	0.3684	0.2090
	30	5.6639	0.8907	0.4270	0.1922	0.1094
	45	5.1589	0.6304	0.3022	0.1361	0.0775

*The nature of the Lorentz line shape is such that the phase-delay function in the clear air becomes negative above the resonant frequency f_q=22.235 GHz (Liebe, 1969). This trend persists only until higher resonance frequencies are approached and is analagous to the situation for higher frequencies shown in figure 4.

183 and 323 GHz. Further, clouds and precipitation continue to play a significant role. However, the problem of estimating the total attenuation, as in (3), or the total phase delay, as in (4), is currently hampered by the fact that water vapor is the most highly variable constituent of the atmosphere. Further, there are not sufficient data at these frequencies to determine empirically-defined coefficients for vertical structures, such as in (13a). Nevertheless, we can determine the corresponding attenuation and phase delay coefficients (in dB/km and rad/km).

3.1. Clear-Sky Effects

When the dispersive phase-delay coefficient, $\Delta\phi_{N_w}$ in radians/km, caused by water vapor is given by the Lorentz line-shape formula (Liebe, 1969), a simple relationship,

$$\Delta\phi_{N_w}(f) = \Delta\phi_N(f) - \Delta\phi_{N_o}(f) = \frac{(f_o - f)}{8.686}\ \alpha_w(f) \quad . \tag{21}$$

can be established between:

$\alpha_w(f)$, the attenuation coefficient in dB/km;

$\Delta\phi_{N_o}(f)$, the portion of the dispersive phase delay caused by atmospheric oxygen; and

$\Delta\phi_N(f)$, the total dispersive phase-delay coefficients in radians/km.

However, one of the most straightforward formulations for attenuation $\tau_w(f)$ is that of Ulaby and Straiton (1970) who do not use the Lorentz formulation. Instead they use the Van Vleck-Weiskopf line-shape formulation. Nonetheless it is assumed here that the Van Vleck-Weiskopf line-shape formulation for the attenuation of Ulaby and Straiton (1970) can be used in conjunction with (21) to predict $\Delta\phi_{N_w}(f)$ due to water vapor in the 130 to 350 GHz region. The oxygen-caused phase-delay and attenuation coefficients $\Delta\phi_{N_o}(f)$ and $\alpha_o(f)$, can be obtained directly from expressions given by Ott and Thompson (1976).

Therefore, we have established procedures for predicting the values of the $\Delta\phi_N(f)$, the $\alpha_w(f)$, and the $\alpha_o(f)$ for the 50 to 350 GHz frequency region. Figures 3 and 4 show the results of calculations for a location having a surface pressure of 1013.25 mb (sea level), a surface temperature of 20°C, and a surface relative humidity of 43 percent. Figure 3 shows the sum of the two

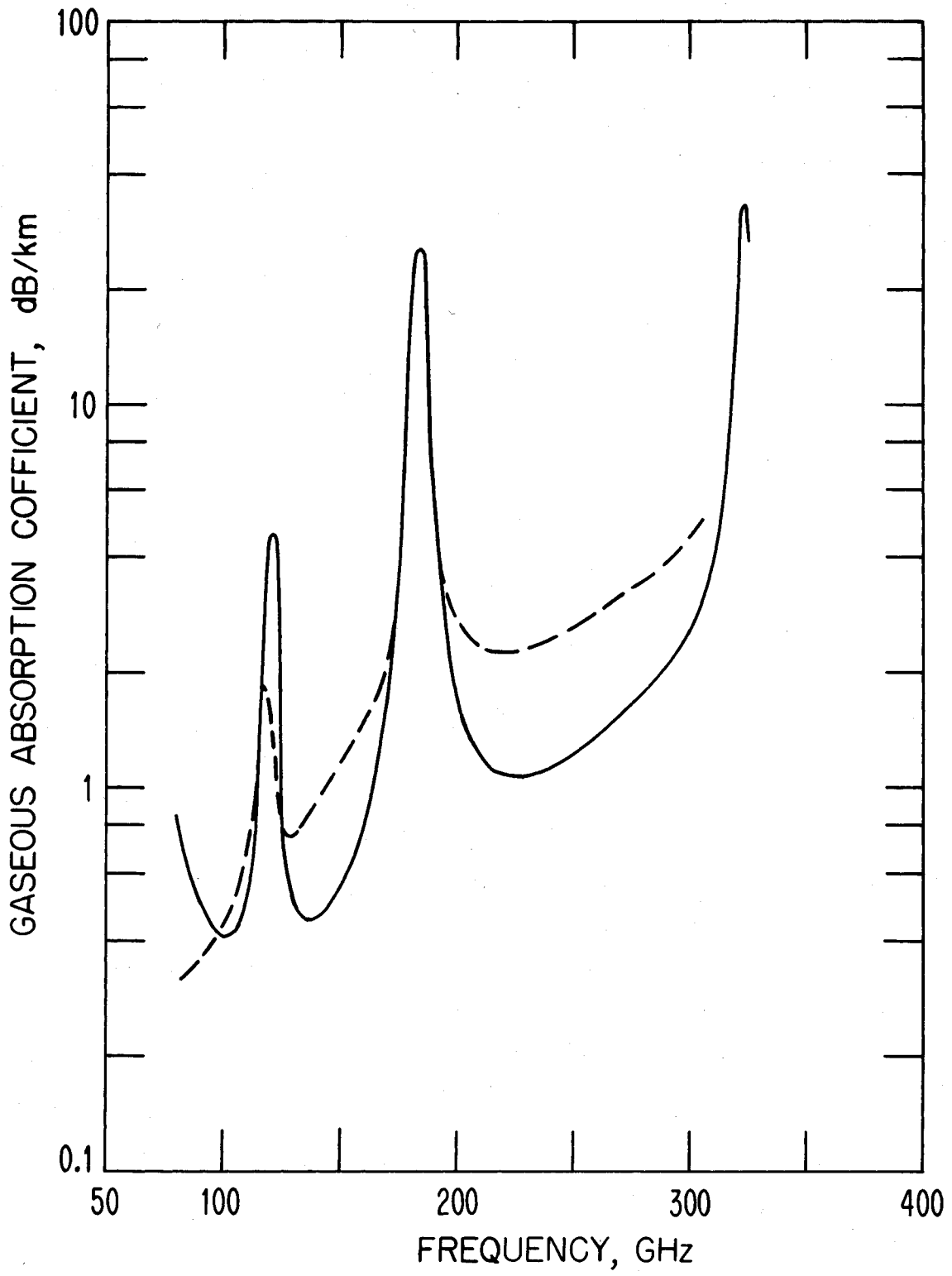

Figure 3. The clear-sky attenuation coefficient (dB/km) due to gaseous absorption (by water vapor and oxygen) at sea level. The temperature is 20°C, the water vapor density is 7.5 g/m³.

attenuations $\alpha_o(f)$ and $\alpha_w(f)$ over a surface link 1 km long; i.e. decibels of attenuation per kilometer versus frequency. Figure 4 shows the dispersive phase delay $\Delta\phi_N(f)$ versus frequency, again over an assumed 1 km surface link (or phase delay in radians per kilometer). Only residual effects of the 60 GHz oxygen resonance are noted in both figures near 80 GHz. Additionally, the two water-vapor resonances have almost the same impact near their respective resonances, whereas the 119 GHz oxygen resonance impact is far less in both figures 3 and 4.

Recently Liebe and Gimmestad (1978) presented a detailed study of clear-sky absorption properties. Their results are included in Figure 3 as a dashed-line curve.

3.2. Cloud Effects

The relatively straightforward formulations of section 2.2 for cloud effects can be used, if we are in the so-called "Rayleigh" frequency region (Bean et al., 1970). However, if we are in the "Mie" region, the calculations become vastly more complicated. The Rayleigh approximations are roughly applicable when

$$\rho f < 0.4 \quad , \tag{22}$$

where ρ is a precipitation drop (assumed spherical) radius in centimeters and f is the radio frequency in gigahertz. For clouds, the situation is ameliorated to mainly Rayleigh-region computations, provided (9a) is assumed. Furthermore, if the largest frequency considered, 350 GHz, is used in (22), then a radius $\rho = 11.4\ \mu$ is obtained. Combining this result with (9a), (9b), (9c), and (22), yields the result that approximately 96 percent of all the cloud droplets satisfy (22), even at 350 GHz. The percentage would be larger at lower frequencies. This implies that for even the thickest clouds (with greater percentages of large drops) and highest frequencies, the Rayleigh region can be assumed to hold for cloud-effect computations.

The attenuation coefficient $\alpha_c(f)$ and the phase delay coefficient $\phi_c(f)$ from (10) and (19b) are applicable through 350 GHz. Table III list some typical values.

As mentioned previously in Section 2.2, Goldstein (1951) presented the Debye formula as a good fit to data for frequencies up to about 30 GHz and

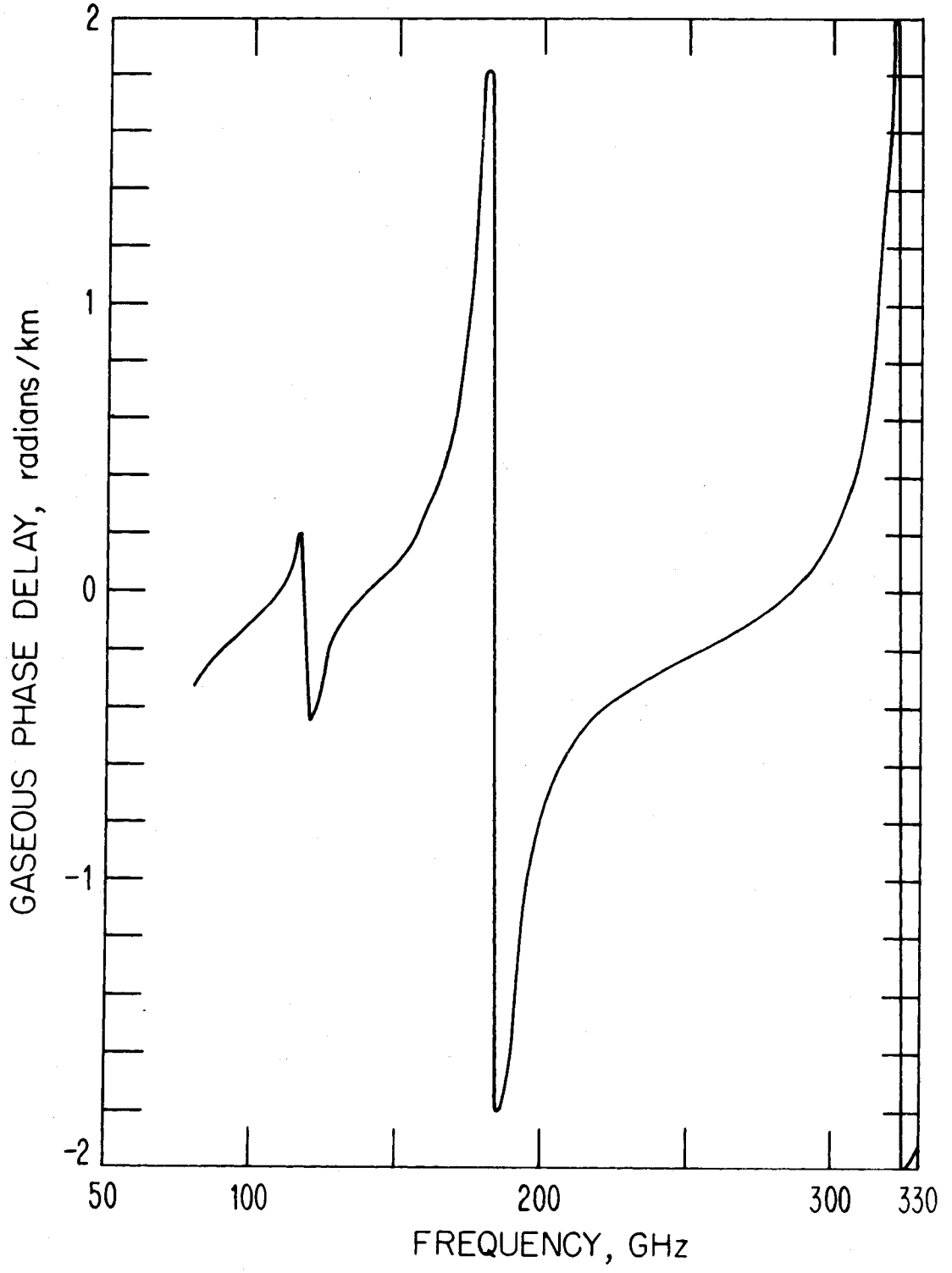

Figure 4. The clear-sky dispersive phase-delay coefficient (rad/km) due to gaseous absorption (by water vapor and oxygen) at sea level. The temperature is 20°C, and the water vapor density is 7.5 g/m^3.

TABLE III

Attenuation And Phase Delay Coefficients
Due To Clouds At 30°C

Frequency, f (GHz)	$\alpha_c(f)$ (dB/km)	$\alpha_c(f)$ (rad./km)
10	0.0211	0.0176
80	1.43	1.61
100	2.14	1.98
200	6.39	3.61
300	10.1	4.96
350	11.5	5.58

As mentioned previously in Section 2.2, Goldstein (1951) presented the Debye formula as a good fit to data for frequencies up to about 30 GHz and Ray (1972) has essentially "blended in" the EHF region by joining the optical and SHF results. These refractive index results are illustrated in Figure 5 for a droplet temperature of 30°C. The dashed lines are Ray's (1972) results, and the solid lines are obtained from the Debye formula using Goldstein's (1951) constants. Based on Ray's (1972) work, then, it has been assumed in the cloud and rain effects computations made herein that the Debye formulation for the dielectric constant of water applies from 80 to 350 GHz.

3.3 Rain Effects

Rain effects at microwave frequencies have been hypothesized and reported at length (Dutton and Dougherty, 1973; Bean and Dutton, 1976; Dutton, 1977 a and b), but these studies have been restricted to frequencies below 50 GHz. It was concluded in section 4.3 that cloud impact on the direct transmission, as given by the simple transfer function (1), could be treated by the Rayleigh approximation (21). A similar assumption had been made in most of the rain studies at SHF mentioned above. However, for rain studies at EHF, the complete Mie formulations for raindrop scattering functions (Zuffery, 1972) must be used. This has a profound impact on the magnitude of these effects, which will be discussed in the following, as each effect is considered individually.

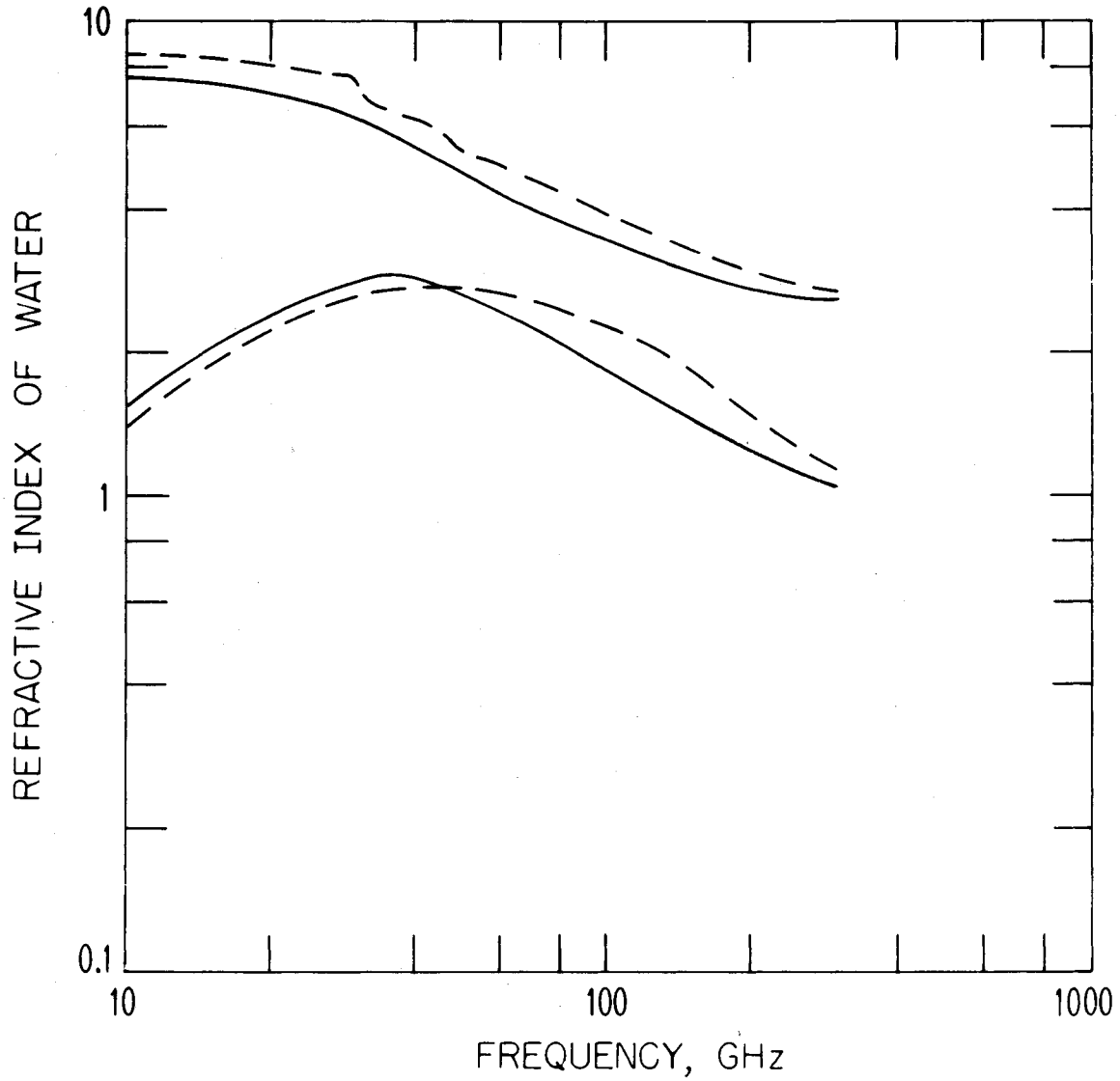

Figure 5. The complex refractive index of water versus frequency. The upper pair of curves are for the real term m'; the lower pair of curves are for the imaginary term m". The dashed-line curves were determined by the Debye model (Goldstein, 1951); the solid-line curves were determined from Ray's model (1972).

3.3.1. Phase Delay By Rainfall

From the classic Mie (1908) theory, Zuffery (1972) develops what is known as the "forward scatter function" of a spherical water droplet impinged by electromagnetic radiation. In an earlier expression, (12a), we introduced the complex refractive index, m, of a water droplet. Through an infinite series representation involving spherical Bessel and Hankel functions, the m is related to the forward scattering function. When several of these water droplets are assumed randomly "embedded" in a slab of the atmospheric medium of length $d\ell$, the "equivalent" (or essentially average) increase, $m_e(f)$, of the refractive index of the medium over that for clear air can be obtained by integrating over the forward scattering functions of all droplets in the slab.

The reader interested in the theoretical development is referred to reports such as that by Rogers and Olsen (1976). The increase in the complex index of refraction, $m_e(f)$, can be expressed as

$$m_e(f) = m_e'(f) - im_e''(f) \quad . \tag{23}$$

The real part of (23), $m_e'(f)$, is directly related to the rain-caused phase delay, $\Phi_p(f)$ in (4), by

$$\Phi_p(f) = 10^{-6}\, k_o \int_o^{\ell} m_e'(f)\, d\ell \quad ,$$

where, again, k_o is the free-space wavenumber at frequency f, $\Phi_p(f)$ is in radians, and $d\ell$ is the differential path length increment.

Results for a 1 km link with a surface rain rate of 60 mm/hr, a surface temperature of 15°C, a surface pressure of 1000 mn, and a surface relative humidity of 60° (roughly Washington, DC, for a .01% of an average year) are shown in Figure 6. The dropsize distribution used to determine $\phi_p(f)$ is the modified Marshall-Palmer distribution described in Section 2.3. The results, unlike results at SHF, indicate that the phase-delay coefficient due to precipitation, $\phi_p(f)$ in rad/km, decreases rather dramatically with frequency. Recalling Table III, the results for clouds increase with frequency rather dramatically, implying that, at higher frequencies, the cloud effects could indeed be the more important of the two as far as phase delay is concerned.

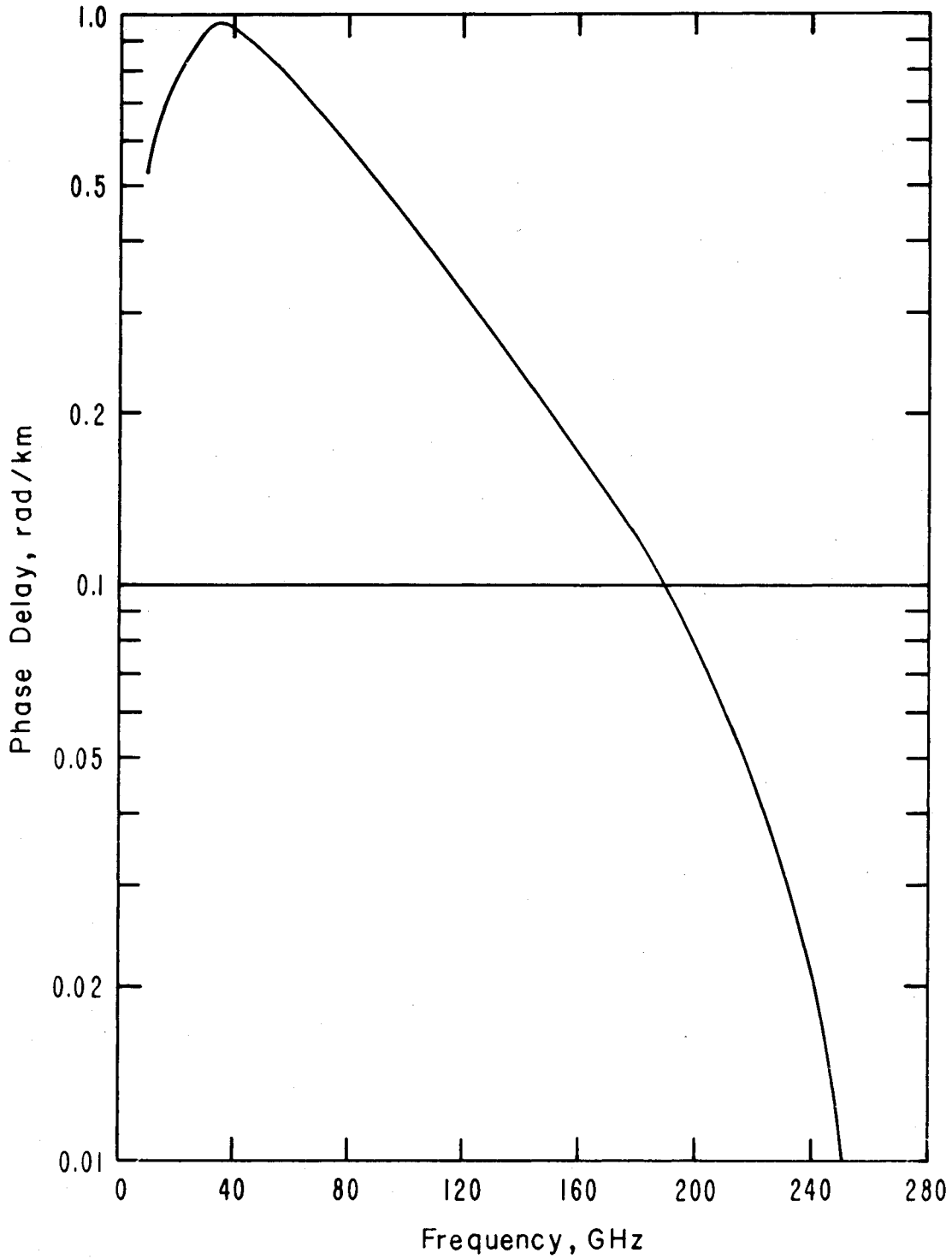

Figure 6. The dispersive phase-delay coefficient (rad/km) due to rainfall (60 mm/hr) for 0.01% of an average year at Washington, DC. The surface pressure, temperature, and relative humidity are, respectively 1000 mb, 15°C, and 60%.

3.3.2. Attenuation By Rainfall

The imaginary part of (23), $m''_e(f)$, is related to the rain-caused attenuation, $\tau_p(f)$, in (3) by

$$\tau_p(f) = 1.82042 \times 10^{-5} \, f \int_0^{\ell} m''_e(f) \, d\ell \quad , \tag{25}$$

where f is the frequency in gigahertz. Figure 7 shows this attenuation for a 1 km link and the same conditions as in Figure 6; the values are plotted from 10 to 300 GHz on the curve labeled 2. For the range 10 to 95 GHz, there is a curve of attenuation labeled 1, based on the empirical SHF techniques used in section 2.3. The two curves correspond reasonably closely to about 80 GHz, but then, at least for the remaining 15 GHz in common, the two curves begin to diverge. Values from the theoretical curve labeled 2 thereafter tend to plateau beyond 95 GHz and even to decrease slightly above about 150 GHz. Rain attenuation remains a more dominant effect than cloud attenuation. This is in contrast with the situation observed in the previous section on phase delay.

4. CONCLUSION

The simple atmospheric channel transfer function has been estimated for the frequency range of 10 to 350 GHz. This has included the resonance effects of the five prominant molecular resonances, two due to oxygen (in the vicinitities of 60 and 119 GHz) and three due to water vapor (in the vicinities of 22, 183, and 323 GHz). For frequencies below about 120 GHz, there is sufficient empirical data and developed theory to permit estimates of the transfer function for both terrestrial and earth/space systems. See Figures 1 and 2 and Tables I and II.

At higher frequencies, the clear-sky attenuation and phase is primarily due to absorption by water vapor. This is the most variable constituent (temporally and spatially) of the gaseous atmosphere. Further its significance for microwaves (attenuation and phase delay) is dependent upon pressure and temperature, which are also highly variable conditions in the atmosphere. See Figures 3 and 4.

The attenuation and phase delay by clouds are determined from relatively straightforward Rayleigh-region formulation, increasing monotonically with frequency over the range from 10 to 350 GHz. See Table III.

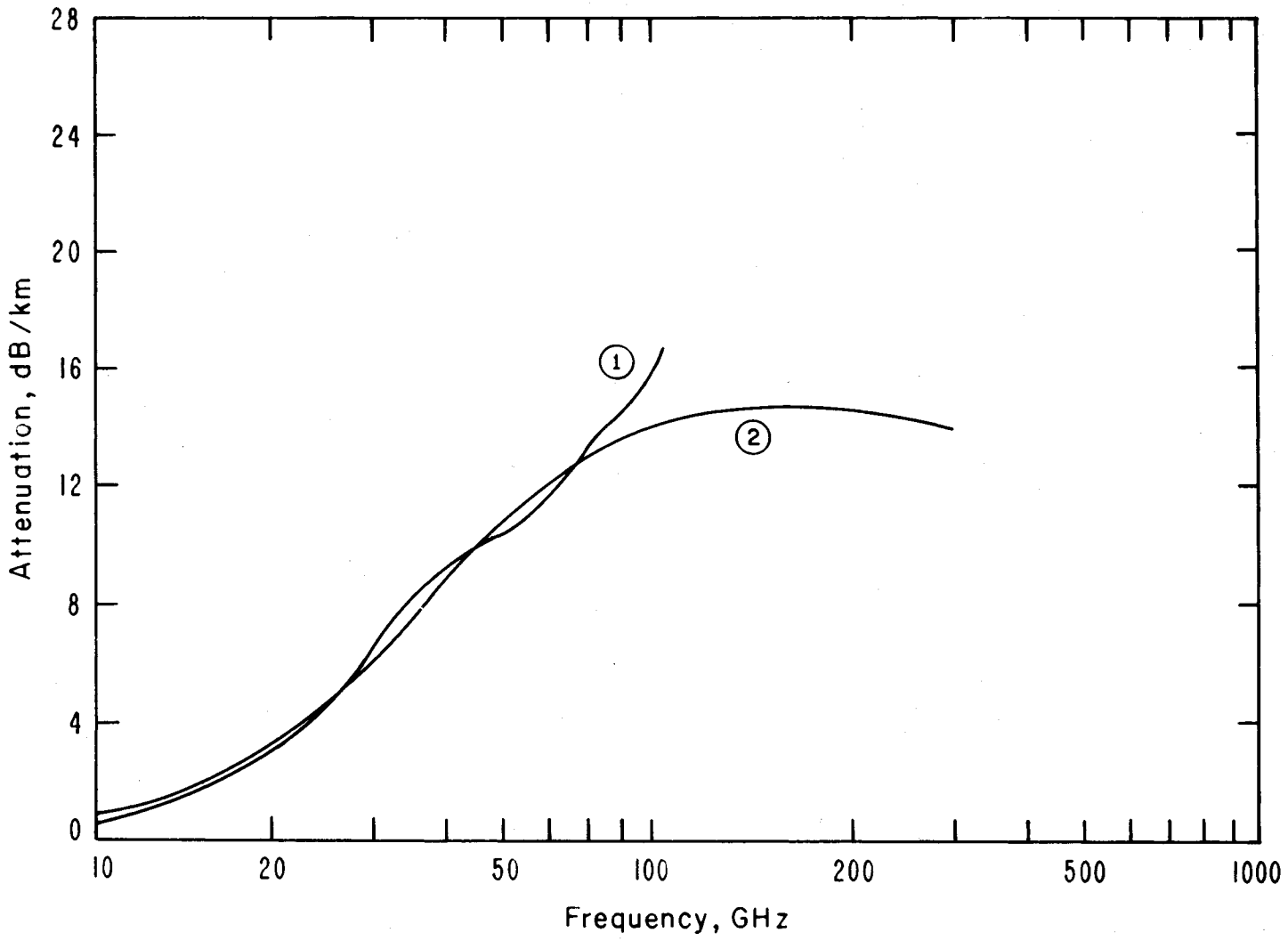

Figure 7. The attenuation coefficient (dB/km) for rainfall (60 mm/hr) for 0.01% of an average year at Wash., DC. The conditions are as for Figure 6. The curve labeled 1 is based upon empirical formulations of the vertical structure. The curve labeled 2 is theoretical.

The attenuation by rainfall, which tend to increase monotonically with frequency to about 80 GHz, plateaus over the region of 80 to 350 GHz. See Figures 2 and 7. However, the phase delay of microwaves caused by rainfall appears to peak at about 35 GHz and then decrease monotonically with frequency thereafter (see Figure 6).

5. REFERENCES

Bean, B. R., and E. J. Dutton (1968), Radio Meteorology (Dover Publications, Inc., New York).

Bean, B. R., and E. J. Dutton (1976), Radiometeorological parameters and climatology, Telecomm. Journal 43, No. VI, June, pp. 427-435.

Bean, B. R., E. J. Dutton, and B. D. Warner (1970), Weather effects on radar, Chap. 24 of Radar Handbook, M. I. Skolnik, editor (McGraw-Hill Book Co., Inc., New York, NY).

Bean, B. R., and G. D. Thayer (1963), Comparison of observed atmospheric radio refraction effects with values predicted through the use of surface observations, NBS J. of Res., Radio Propagation 67D, No. 3, May-June, pp. 273-285.

CCIR (1978), Attenuation By Atmospheric Gases, Report of Vol. V, Propagation In Non-Ionized Media, of the CCIR XIV Plenary Assembly, Kyoto, Japan.

Crane, R. K. (1966), Microwave scattering parameters for New England rain, MIT Lincoln Labs., Lexington, MA, Tech. Rept. 426 Oct. (AD No. 647-798, NTIS, Springfield, VA).

Diermendjian, D. (1963), Complete microwave scattering and extinction properties of polydispersed cloud and rain elements, Report R-422-PR, The Rand Corporation, Santa Monica, CA, Dec.

Dougherty, H. T., and E. J. Dutton (1978), Estimating the year-to-year variability of rainfall for microwave applications, IEEE Trans. Comm. COM-26, No. 8, August.

Dutton, E. J. (1967), Estimation of radio ray attenuation in convective rainfalls, J. Applied Meteorology 6, No. 4, August, pp. 662-668.

Dutton, E. J. (1968), Radio climatology for precipitation and clouds in central Europe, U.S. Dept. of Commerce, ESSA Tech. Rept. ERL68-WPL 3, April.

Dutton, E. J. (1971), A Meteorological Model For Use In The Study Of Rainfall Effects On Atmospheric Radio Telecommunications, Office of Telecomm. OT/TRER-24 (Access No. COM 75-10826/AS, NTIS, Springfield, VA).

Dutton, E. J. (1977a), Earth-space attenuation prediction procedures at 4 to 16 GHz, Office of Telecomm. Report OTR 77-123, May (Access No. PB269228/AS, NTIS, Springfield, VA).

Dutton, E. J. (1977b), Precipitation visiability in the USA for microwave terrestrial system design, OT Report OTR 77-134, November (Access No. A049041, NTIS, Springfield, VA).

Dutton, E. J., and H. T. Dougherty (1973), Modeling the effects of clouds and rain upon satellite-to-ground system performance, Office of Telecomm. Report OTR 73-5, March, (Access No. COM 75-10950/AS, NTIS, Springfield, VA).

Dutton, E. J., and H. T. Dougherty (1979), Year-to-year variability and rainfall for microwave applications in the USA, submitted to IEEE Trans. Comm. COM-27.

Dutton, E. J., H. T. Dougherty, and R. F. Martin, Jr., (1974), Prediction of European Rainfall And Link Coefficients At 8 to 30 GHz, (Access No. A-000804, NTIS, Springfield, VA).

Goldstein, H. (1951), Attenuation by condensed water, in Propagation of Short Radio Waves, D. E. Kerr, ed., MIT Radiation Laboratory Series, 13 (McGraw-Hill Book Co., Inc., New York, NY) pp. 671-692.

Grantham, D. D., and A. J. Kantor (1967), Distribution of radar echoes over the United States, Air Force Surveys In Geophysics, No. 191, AFCRL-67-0232, Air Force Cambridge Res. Labs., Cambridge, Mass. (Access No. 636310, NTIS, Springfield, VA).

Ishimaru, A. (1972), Temporal frequency spectra of multifrequency waves in a turbulent atmosphere, IEEE Trans. Ant. Prop. AP-20, No. 1, January, pp. 10-19.

Liebe, H. J. (1969), Calculated tropospheric dispersion and absorption due to the 22-GHz water vapor line, IEEE Trans. Ant. Prop. AP-17, No. 5, September, pp. 621-627.

Liebe, H. J., and G. G. Gimmestad (1978), Calculation of clear-air EHF refractivity, Radio Sci. 13, No. 2, March-April, pp. 245-252.

Liebe, H. J., and J. D. Hopponen (1977), Variability of EHF air refractivity with respect to temperature, pressure, and frequency, IEEE Trans. Ant. Prop. AP-25, No. 3, May, pp. 336-376.

Liebe, H. J., G. G. Gimmestad, and J. D. Hopponen (1977), Atmospheric oxygen microwave spectrum-experiment versus theory, IEEE Trans., Ant. Prop. AP-25, No. 3, May, pp. 327-335.

Linfield, R. F. (1977), Radio channel capacity limitations, Office of Telecomm. Report OTR 77-132, November. (Access No. PB275239/AS, NTIS, Springfield, VA).

Lukes, G. D. (1968), Penetrability of haze, fog, clouds and precipitation by radiant energy over the spectral range 0.1 micron to 10 centimeters, Center for Naval Analysis, Naval Warfare Analysis Group Study 61, Univ. of Rochester, Arlington, VA, May (Access No. PB275239/AS, NTIS, Springfield, VA).

Marshall, J. S., and W. McK. Palmer (1948), The distribution of raindrops with size, J. Meteorology 5, p. 165.

Mie, G. (1908), Beitruge zur optik truber medien, speziell kolloidaler metallasungen, Annalen der Physik 25, March, pp. 377-445.

Ott, R. H., and M. C. Thompson, Jr. (1976), Characteristics of a radio link in the 55 to 65 GHz range, IEEE Trans. Ant. Prop. AP-24, No. 6, November, pp. 873-877.

Ray, P. S. (1972), Broadband complex refractive indices of ice and water, J. Applied Optics, 11, No. 8, August, pp. 1836-1844.

Rice, P. L., and N. R. Holmberg (1973), "Cumulative time statistics of surface point-rainfall rates", IEEE Trans. Commun. COM-21,No. 10, October, pp. 1131-1136.

Rogers, D. V., and R. L. Olsen (1976), Calculation of radiowave attenuation due to rain at frequencies up to 1000 GHz, Report CRC No. 1299, Communications Research Centre, Dept. of Communications, Ottawa, Canada, November.

Ulaby, F. T., and A. W. Straiton (1970), Atmospheric absorption of radio links in the 55 to 65 GHz range, IEEE Trans. Ant. Prop. AP-24, No. 4, July, pp. 479-485.

Van Vleck, J. H. (1947a), The absorption of microwaves by oxygen, Phys. Rev. 71, pp. 425-433.

Van Vleck, J. H. (1947b), The absorption of microwaves by uncondensed water, Phys. Rev. 71, pp. 425-433.

Zuffery, C. H. (1972), A study of rain effects on electromagnetic waves in the 1-600 GHz range, Univ. of Colorado, Dept. of Elec. Engineering thesis.

FORM OT-29
(3-73)

U.S. DEPARTMENT OF COMMERCE
OFFICE OF TELECOMMUNICATIONS

BIBLIOGRAPHIC DATA SHEET

	1. PUBLICATION OR REPORT NO. NTIA Report 78-8	2. Gov't Accession No.
3. Recipient's Accession No.		
4. TITLE AND SUBTITLE ESTIMATES OF THE ATMOSPHERIC TRANSFER FUNCTION AT SHF AND EHF		5. Publication Date August 1978
		6. Performing Organization Code NTIA/ITS
7. AUTHOR(S) E. J. Dutton and H. T. Dougherty		9. Project/Task/Work Unit No.
8. PERFORMING ORGANIZATION NAME AND ADDRESS National Telecommunications & Information Administration Institute for Telecommunication Sciences Boulder, CO 80303		10. Contract/Grant No.
11. Sponsoring Organization Name and Address		12. Type of Report and Period Covered
		13.

14. SUPPLEMENTARY NOTES

15. ABSTRACT *(A 200-word or less factual summary of most significant information. If document includes a significant bibliography or literature survey, mention it here.)*

Known theory is applied to examine the channel transfer function for earth/space propagation paths through the atmosphere and over the frequency range from 10 to 350 GHz. The associated attenuation and phase-delay characteristics are separated into the contributions of the clear-sky, clouds, and rainfall. From the available meteorological data, the total path attenuation and phase-delay is estimated over the frequency range from 10 to 45 GHz for selected values of the initial elevation angles from a ground station near Washington, DC.

The associated attenuation coefficients (dB/km) and phase-delay coefficients (rad/km) attributable to the clear air, clouds, and rainfall are also described for frequencies up to 350 GHz.

16. Key words *(Alphabetical order, separated by semicolons)*

Atmospheric attenuation, atmospheric phase delay, clear-air effects, effects of clouds, effects of rainfall, microwave frequencies, millimeter waves.

17. AVAILABILITY STATEMENT ☒ UNLIMITED. ☐ FOR OFFICIAL DISTRIBUTION.	18. Security Class *(This report)* Unclassified	20. Number of pages 29
	19. Security Class *(This page)* Unclassified	21. Price:

☆GOVERNMENT PRINTING OFFICE: 1978—779-042/31 REGION NO. 8

USCOMM-DC 29716-P73
USCOMM - ERL